




ORIGINAL

## Adaptive Multi-Scale Contrast Enhancement and Morphological Flow Integration for Diabetic Retinopathy Detection Using ELM-Based Classifier

### Mejora adaptativa del contraste multiescala e integración del flujo morfológico para la detección de la retinopatía diabética mediante clasificadores basados en ELM

Basma Esserkassi<sup>1</sup> , Zaynab Boujelb<sup>2</sup> , Souad Eddarouich<sup>3</sup> , Abdennaser Bourouhou<sup>1</sup>

<sup>1</sup>ENSAM, E2SN, Mohammed V University. Rabat, Morocco.

<sup>2</sup>Faculty of Sciences, Ibn Tofail University. Kenitra, Morocco.

<sup>3</sup>Regional Educational Center. Rabat, Morocco.

**Cite as:** Esserkassi B, Boujelb Z, Eddarouich S, Bourouhou A. Adaptive Multi-Scale Contrast Enhancement and Morphological Flow Integration for Diabetic Retinopathy Detection Using ELM-Based Classifier. Data and Metadata. 2025; 4:1220. <https://doi.org/10.56294/dm20251220>

Submitted: 06-04-2025

Revised: 09-07-2025

Accepted: 20-10-2025

Published: 21-10-2025

Editor: Dr. Adrián Alejandro Vitón Castillo 

Corresponding Author: Basma Esserkassi 

#### ABSTRACT

**Introduction:** diabetic retinopathy affects 100 million individuals worldwide and represents a leading preventable cause of vision loss. Automated screening systems demonstrate suboptimal performance due to heterogeneous imaging conditions and insufficient preprocessing strategies. This study aimed to develop an integrated artificial intelligence pipeline that combines adaptive preprocessing, morphological feature extraction, and optimized classification methods for robust diabetic retinopathy severity assessment.

**Method:** the research employed the preprocessed “Diabetic Retinopathy Arranged” dataset from Kaggle platform containing 34 860 fundus images across five severity grades. Three methodological innovations were implemented: Adaptive Multi-Scale Contrast Limited Adaptive Histogram Equalization (AMS-CLAHE) for content-aware preprocessing, Morphological Transition Flow architecture for structural change modeling, and Bayesian optimization for Extreme Learning Machine variants. Comprehensive ablation studies evaluated preprocessing configurations, architectural components, and classification strategies through systematic parameter optimization.

**Results:** the study proposes an AMS-CLAHE framework with dynamic threshold calibration and entropy-based attention mechanisms for content-aware preprocessing, achieving F1-score of 0,908 and AUC-ROC of 0,986 with processing efficiency below 250ms per image. The All-ELM configuration demonstrated superior performance (F1=0,970, accuracy=0,970) compared to conventional architectures. LAB color space processing outperformed RGB representation. Bayesian-optimized Random Forest delivered optimal classification results (F1=0,997, MCC=0,996) across all severity grades.

**Conclusions:** the integrated pipeline demonstrated that systematic preprocessing optimization enables competitive diagnostic accuracy while maintaining computational efficiency. This approach facilitates scalable diabetic retinopathy screening implementation in diverse clinical environments where expert assessment remains limited.

**Keywords:** Diabetic Retinopathy; Adaptive Preprocessing; Morphological Feature Extraction; Extreme Learning Machines; Bayesian Optimization; Multi-Channel Processing.

#### RESUMEN

**Introducción:** la retinopatía diabética afecta a 100 millones de personas en todo el mundo y representa una de las principales causas prevenibles de pérdida de visión. Los sistemas de cribado automatizados presentan

un rendimiento subóptimo debido a la heterogeneidad de las condiciones de imagen y a estrategias de preprocesamiento insuficientes. Este estudio tuvo como objetivo desarrollar un proceso integrado de inteligencia artificial que combina preprocesamiento adaptativo, extracción de características morfológicas y métodos de clasificación optimizados para una evaluación robusta de la gravedad de la retinopatía diabética. **Método:** la investigación empleó el conjunto de datos preprocesado “Diabetic Retinopathy Arranged” de la plataforma Kaggle, que contiene 34 860 imágenes de fondo de ojo en cinco grados de gravedad. Se implementaron tres innovaciones metodológicas: Ecuilibración de Histograma Adaptativo Limitado por Contraste Multiescala Adaptativo (AMS-CLAHE) para el preprocesamiento basado en el contenido, arquitectura de Flujo de Transición Morfológica para el modelado de cambios estructurales y optimización bayesiana para variantes de la Máquina de Aprendizaje Extremo. Estudios exhaustivos de ablación evaluaron las configuraciones de preprocesamiento, los componentes arquitectónicos y las estrategias de clasificación mediante la optimización sistemática de parámetros.

**Resultados:** el estudio propone un marco AMS-CLAHE con calibración dinámica de umbrales y mecanismos de atención basados en la entropía para el preprocesamiento basado en el contenido, logrando una puntuación F1 de 0,908 y un AUC-ROC de 0,986 con una eficiencia de procesamiento inferior a 250 ms por imagen. La configuración All-ELM demostró un rendimiento superior ( $F1 = 0,970$ , precisión = 0,970) en comparación con las arquitecturas convencionales. El procesamiento del espacio de color LAB superó la representación RGB. El Bosque Aleatorio optimizado bayesiano proporcionó resultados de clasificación óptimos ( $F1 = 0,997$ ,  $MCC = 0,996$ ) en todos los grados de gravedad.

**Conclusiones:** el proceso integrado demostró que la optimización sistemática del preprocesamiento permite una precisión diagnóstica competitiva, manteniendo al mismo tiempo la eficiencia computacional. Este enfoque facilita la implementación escalable del cribado de la retinopatía diabética en diversos entornos clínicos donde la evaluación experta sigue siendo limitada.

**Palabras clave:** Retinopatía Diabética; Preprocesamiento Adaptativo; Extracción de Características Morfológicas; Máquinas de Aprendizaje Extremo; Optimización Bayesiana; Procesamiento Multicanal.

## INTRODUCTION

Diabetes mellitus has emerged as one of the most pressing global health challenges of the 21st century, affecting an estimated 589 million adults worldwide as of 2024, with projections indicating a rise to 853 million by 2050.<sup>(1)</sup> This metabolic disorder fundamentally disrupts glucose homeostasis, leading to chronic hyperglycemia that progressively damages multiple organ systems. The pathophysiological cascade begins with insulin resistance or deficiency, resulting in sustained elevation of blood glucose levels that trigger oxidative stress, inflammatory responses, and endothelial dysfunction across vascular networks. The disease's complexity extends beyond its immediate metabolic effects, encompassing a spectrum of microvascular and macrovascular complications that impact patient quality of life and impose substantial economic burdens on healthcare systems globally.<sup>(2)</sup>

Among the constellation of diabetic complications, diabetic retinopathy (DR) represents the most prevalent microvascular complication, with global prevalence estimates indicating that 22,27 % of individuals with diabetes develop some form of retinopathy, while 6,17 % progress to vision-threatening stages.<sup>(3)</sup> The condition constitutes the leading cause of preventable blindness among working-age adults, with particularly high prevalence rates documented in Africa (35,90 %) and North America (33,30 %).<sup>(3)</sup> The pathophysiology of DR involves a complex cascade of retinal vascular changes initiated by prolonged hyperglycemia, including pericyte loss, basement membrane thickening, and breakdown of the blood-retinal barrier. These early molecular changes progress through distinct clinical stages, from mild nonproliferative retinopathy characterized by microaneurysms and dot hemorrhages, to severe proliferative disease marked by neovascularization, vitreous hemorrhage, and tractional retinal detachment.<sup>(4)</sup>

The clinical impact of DR extends far beyond visual impairment, with profound consequences for patients' daily functioning and psychological well-being. Systematic reviews document that diabetic retinopathy limits essential activities including working, driving, walking, reading, and diabetes self-management tasks such as insulin preparation and glucose monitoring.<sup>(5)</sup> Patients experience substantial restrictions in mobility and increased fear of accidents, with driving limitations having pervasive effects on transport, social life, relationships, work responsibilities, and independence. The psychological burden is equally significant, with patients reporting frustration due to visual restrictions, anxiety about further vision loss, and difficulty coping with diagnostic uncertainty. Employment capacity becomes compromised, particularly in visually demanding occupations, while social isolation increases as patients withdraw from activities they can no longer safely

perform. The economic implications include both direct healthcare costs and indirect costs related to reduced productivity and increased dependency on caregivers.<sup>(5)</sup>

The evolution of DR detection methodologies has undergone significant transformation over the past two decades, driven by technological advances and the pressing need for scalable screening solutions. Traditional ophthalmoscopic examination, encompassing both direct and indirect ophthalmoscopy performed through dilated pupils, remains the clinical gold standard for comprehensive retinal evaluation. Direct ophthalmoscopy provides detailed visualization of central retinal features but offers limited peripheral assessment, while indirect ophthalmoscopy enables broader retinal examination with stereoscopic visualization capabilities. However, these examination techniques face substantial implementation challenges in diverse healthcare environments, particularly regarding resource allocation, workflow integration, and the requirement for specialized expertise.<sup>(6)</sup>

The advent of digital fundus photography in the early 2000s marked a pivotal advancement in DR screening methodology. Mydriatic fundus photography, requiring pharmacological pupil dilation, provides high-quality images suitable for detailed grading but introduces workflow complexity and patient discomfort. Non-mydriatic systems offer improved patient acceptance and workflow efficiency but may compromise image quality in eyes with small pupils or media opacities. Recent technological developments include ultra-widefield imaging systems that capture up to 200 degrees of retinal coverage in a single image, enabling comprehensive peripheral retinal assessment crucial for detecting ischemic changes and neovascularization.<sup>(7)</sup> Smartphone-based imaging platforms have emerged as cost-effective solutions for resource-limited settings, though image quality limitations remain a concern for accurate DR grading.<sup>(7)</sup>

Advanced imaging modalities have further enhanced diagnostic capabilities. Fluorescein angiography remains the gold standard for evaluating retinal vascular perfusion and diagnosing macular ischemia, revealing microaneurysms, areas of nonperfusion, and abnormal vessel leakage through sodium fluorescein dye injection.<sup>(8)</sup> However, its invasive nature and potential adverse effects limit routine use. Optical coherence tomography (OCT) provides high-resolution, three-dimensional retinal imaging enabling quantitative assessment of macular thickness and early detection of subclinical macular edema missed by traditional examination methods.<sup>(8)</sup> OCT angiography represents a significant advancement, offering non-invasive visualization of retinal microvasculature through motion contrast imaging, enabling detailed assessment of capillary perfusion without dye injection.<sup>(9)</sup>

The integration of artificial intelligence into ophthalmology has fundamentally altered the landscape of DR detection, with machine learning models demonstrating significant advances in medical image analysis across multiple clinical applications.<sup>(10)</sup> Recent developments have shown the evolution from traditional computational approaches to sophisticated transformer-based models that enable unified processing of multimodal diagnostic inputs.<sup>(11)</sup> Despite this technological progress, contemporary AI systems face persistent challenges that limit their clinical translation. Medical imaging data preparation remains complex, with studies indicating substantial variations in image quality and standardization requirements across different clinical environments, affecting 20 % of images in automated screening programs.<sup>(12)</sup>

Current automated classification approaches exhibit fundamental limitations that constrain their clinical effectiveness. Empirical evaluations of preprocessing methods reveal significant performance variations when comparing different enhancement techniques across multiple imaging modalities, highlighting the need for adaptive approaches that can accommodate diverse imaging conditions.<sup>(13)</sup> Standard contrast enhancement methods fail to account for subtle pathological differences or varying illumination conditions, potentially obscuring critical diagnostic features or introducing artifacts that compromise classification accuracy. Additionally, recent developments in fundus image enhancement networks demonstrate the technical complexity involved in preserving diagnostic features while improving image quality for automated analysis.<sup>(14)</sup>

The computational demands of contemporary deep learning architectures present barriers to widespread clinical deployment. Image augmentation research has documented the extensive computational requirements associated with modern deep learning pipelines, particularly in medical imaging applications where processing times must be compatible with clinical workflows.<sup>(15)</sup> Furthermore, research on explainability demonstrates that the black-box nature of deep neural networks limits clinical interpretability, creating challenges for physician acceptance and regulatory approval in healthcare applications.<sup>(16)</sup>

Recent advances in extreme learning machines (ELM) have shown promise in diabetic retinopathy classification tasks, with studies demonstrating that parallel convolutional neural network architectures combined with ELM classifiers can achieve competitive performance while addressing computational efficiency concerns.<sup>(17)</sup> These single-layer feedforward architectures offer rapid training capabilities and reduced computational overhead compared to traditional deep learning approaches. Simultaneously, developments in enhanced feature extraction networks for medical image segmentation provide opportunities to improve diagnostic accuracy while maintaining processing efficiency.<sup>(18)</sup>

The convergence of these methodological advances creates unprecedented opportunities for developing clinically deployable DR detection systems. The clinical imperative for improved DR screening systems continues to grow with the global diabetes epidemic, as early detection and timely intervention can prevent or delay vision-

threatening complications in up to 90 % of cases. Current screening coverage remains inadequate, particularly in underserved populations where access to specialized care is limited.<sup>(19)</sup> The integration of artificial intelligence in healthcare shows promise for revolutionizing patient care through enhanced diagnostic capabilities and decision support systems that can bridge the gap between clinical need and resource availability.<sup>(20)</sup>

Automated systems that effectively balance diagnostic accuracy with computational efficiency could substantially expand screening accessibility and enable implementation in diverse clinical environments where expert ophthalmological assessment remains limited. Such systems must address the heterogeneity inherent in multi-site clinical imaging while maintaining the precision required for accurate disease severity staging and treatment planning decisions.<sup>(21)</sup>

This research addresses the critical need for robust and efficient diabetic retinopathy (DR) classification systems by developing and validating a comprehensive artificial intelligence tool designed for clinical applicability. The proposed pipeline integrates three methodological innovations: (i) an Adaptive Multi-Scale Contrast Limited Adaptive Histogram Equalization (AMS-CLAHE) framework for content-aware preprocessing under heterogeneous imaging conditions; (ii) a Morphological Transition Flow (MTF) architecture that models dynamic retinal structural changes through iterative morphological operations; and (iii) systematic Bayesian optimization applied to advanced Extreme Learning Machine classifiers and their variants Random Vector Functional Link networks (RVFL) and Broad Learning System (BLS), for data-informed parameter tuning. The primary objective of this study is to demonstrate that this integrated AI tool can achieve high diagnostic accuracy in DR severity classification while maintaining computational efficiency suitable for real-time deployment in diverse healthcare settings.

## METHOD

### *Type of study*

This investigation was conducted as an observational study with a descriptive cross-sectional design. The study focused on developing and validating computational methods for automated disease classification across different severity stages of diabetic retinopathy at a single time point, utilizing pre-existing fundus imaging data without longitudinal follow-up requirements.

### *Universe and Sample*

#### **Target Population and Universe**

The universe encompasses all adult patients with diabetes mellitus who undergo fundus photography screening for diabetic retinopathy detection. This population represents individuals at risk for developing vision-threatening diabetic complications requiring systematic ophthalmological surveillance according to established clinical guidelines.

#### **Study Sample and Sampling Strategy**

The study sample consisted of 34 860 digital fundus photographs obtained from the EyePACS Diabetic Retinopathy Detection dataset, a publicly available collection originally developed for the Kaggle competition platform. This dataset represents a convenience sample derived from the EyePACS telemedicine screening program, which captured images from multiple camera systems across clinical sites in the United States.

### *Sample Characteristics*

- Image Resolution Range: 433×289 to 5184×3456 pixels.
- Acquisition Sources: multiple camera systems across U.S. clinical sites.
- Geographic Distribution: multi-site collection reflecting diverse clinical environments.

### *Variables*

The dependent and independent variables used in this study are detailed below.

#### **Dependent Variable**

- Diabetic Retinopathy Severity Grade: Categorical ordinal variable representing five levels according to International Clinical Diabetic Retinopathy (ICDR) classification:
  1. Grade 0: no diabetic retinopathy.
  2. Grade 1: mild nonproliferative diabetic retinopathy.
  3. Grade 2: moderate nonproliferative diabetic retinopathy.
  4. Grade 3: severe nonproliferative diabetic retinopathy.
  5. Grade 4: proliferative diabetic retinopathy.

**Independent Variables**

- Raw fundus image features: digital pixel intensity values across RGB color channels (continuous variables, range 0-255).
- Enhanced image features: processed pixel values following AMS-CLAHE preprocessing (continuous variables, range 0-1 after normalization).
- Morphological features: structural characteristics extracted through Morphological Transition Flow algorithms.
- Multi-scale features: feature representations derived from different spatial resolution levels.
- Color space representations: RGB, LAB, and HSV color channel configurations.

**Technical Variables**

*Image Processing Parameters*

- Spatial resolution: standardized to 224×224 pixels through bilinear interpolation.
- Enhancement configuration: five systematic AMS-CLAHE parameter sets (categorical variable).
- Channel Processing Strategy: late fusion, early fusion, and standard CNN baseline (categorical variable).

*Algorithm Configuration Variables*

- Network architecture depth: number of convolutional blocks (2-4 blocks, discrete variable).
- ELM classifier type: extreme Learning Machine variants (ELM, RVFL, BLS, categorical variable).
- Feature fusion method: concatenation, averaging, weighted, and attention-based fusion (categorical variable).
- Optimization level: baseline, optimized, high-performance, and Bayesian-optimized (ordinal variable).

**Data Collection and Processing**

**Data Source**

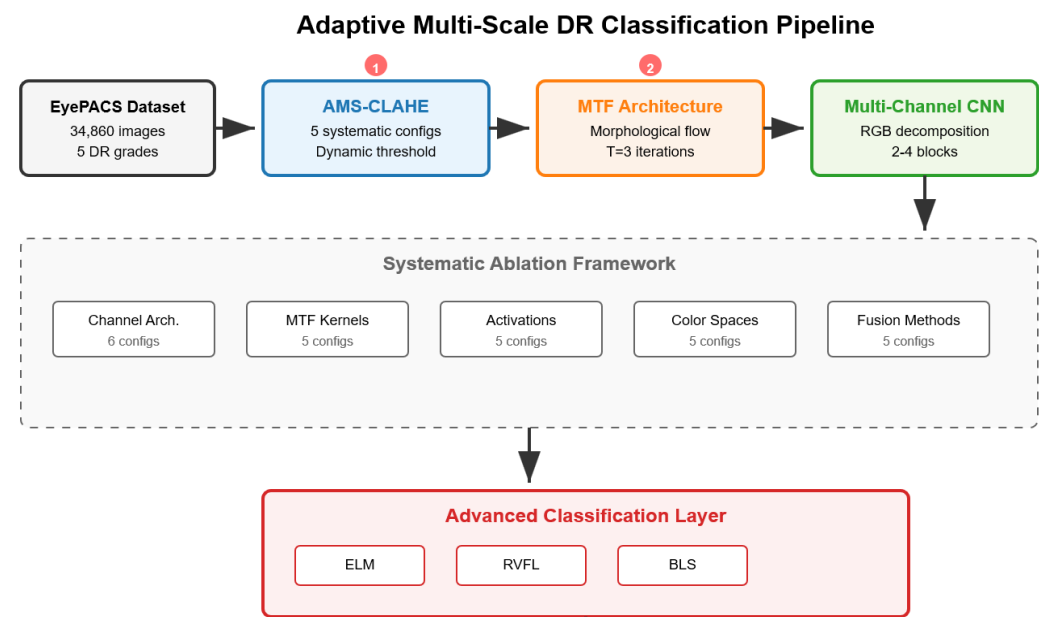
Fundus photographs were sourced from the “Diabetic Retinopathy Arranged” dataset on Kaggle platform<sup>21</sup>, a preprocessed and systematically organized version of the original EyePACS Diabetic Retinopathy Detection competition dataset. The original images were captured as part of routine diabetic retinopathy screening using standardized telemedicine protocols across participating clinical sites.

**Ethical standards**

This study used the open-access Kaggle EyePACS dataset, which contains fully anonymized fundus images collected under institutional approval by its custodians. No identifiable patient information was accessed, and the analysis complies with the Declaration of Helsinki and applicable data protection regulations.

**DEVELOPMENT**

The overall computational architecture is summarized in figure 1.





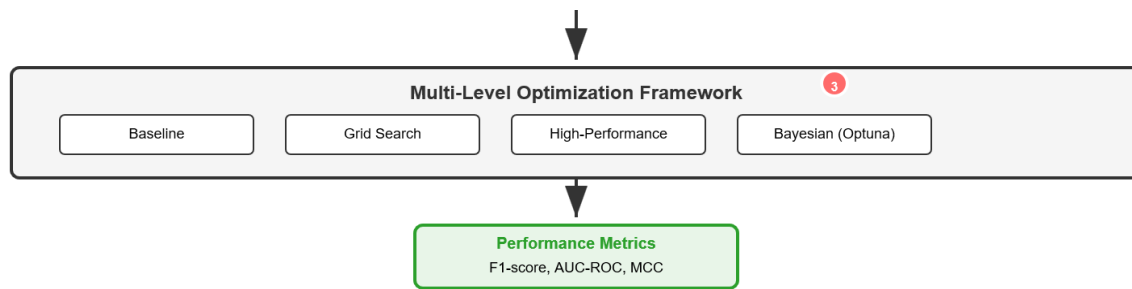


**Figure 1.** Adaptive Multi-Scale Diabetic Retinopathy Classification Pipeline. The framework integrates AMS-CLAHE preprocessing (①), Morphological Transition Flow architecture (②), multi-channel CNN processing with ELM variants, and systematic Bayesian optimization (③). Ablation studies encompass 5 systematic configurations across preprocessing, architectural, and optimization components. Numbers in red circles indicate key methodological innovations

### AMS-CLAHE preprocessing

Building upon the established CLAHE methodology,<sup>(22,23)</sup> a novel AMS-CLAHE framework was developed to address heterogeneous imaging conditions inherent in multi-site clinical datasets. Five systematic enhancement configurations were designed, ranging from baseline configuration to full configuration implementations, each controlled by specific parameter sets enabling rigorous ablation analysis. The framework incorporates dynamic threshold calibration using morphological gradient guidance<sup>(24)</sup> with entropy-driven attention mechanisms for content-aware enhancement while preserving pathological structures essential for diabetic retinopathy assessment.<sup>(25)</sup>

### Morphological Transition Flow architecture

The enhanced morphological layer implemented Morphological Transition Flow (MTF) algorithm modeling dynamic evolution of retinal structures through iterative operations:<sup>(26,27)</sup>

$$Flow_{\{t+1\}} = Flow_t + w_t \times (\delta(Flow_t) - \varepsilon(Flow_t)) \times 0,5 + 0,1 \times I_{original}$$

Where decay weights capture structural changes across  $T=3$  iterations while preserving fine retinal details essential for severity grading.<sup>(28)</sup>

### Multi-channel CNN processing with ELM variants

Three channel processing strategies were systematically evaluated: late fusion (independent RGB processing), early fusion (joint channel processing), and standard CNN baseline. The convolutional backbone employed modular block-based design with variable depth (2-4 blocks) incorporating residual connections where dimensionally feasible. Extreme Learning Machine variants (ELM, RVFL, BLS) served as final classification layers with nodes ranging 128-1024, optimized through systematic Bayesian frameworks using Optuna TPESampler.

### Multi-level optimization framework

Advanced fusion architectures incorporating attention mechanisms and learnable weighting strategies were implemented to address retinal feature heterogeneity across colorimetric spaces. Feature dimensionality reduction employed intelligent selection algorithms with adaptive thresholding based on dataset characteristics. Multi-level classifier enhancement spanning four optimization paradigms from baseline configurations to advanced Bayesian frameworks, incorporating intelligent SVM replacement strategies and gradient boosting refinements across 39 total experimental configurations.

### Evaluation and validation

- Primary outcome: weighted F1-score accounting for class imbalance across DR severity grades.
- Comprehensive metrics: twelve evaluation metrics were computed, including AUC-ROC (one-vs-rest and one-vs-one), Matthews Correlation Coefficient, Cohen's kappa, balanced accuracy, and Brier score loss. Individual per-class performance was reported for each severity level using a precision\_class\_{label} methodology.
- Label reliability and data partitioning: ground-truth reliability was accepted from expert annotations provided within the EyePACS dataset without additional external validation. Data partitioning employed stratified holdout validation (train\_test\_split, random\_state=42) with ablation-specific ratios (60/20/20 % for Ablation 1, adaptive 80-90/10-20 % for Ablation 2, and 80/20 % for Ablation 3). To mitigate class imbalance, RandomOverSampler (random\_state=42) was applied systematically or conditionally when imbalance ratios exceeded 2:1.

- Reproducibility protocol: all stochastic processes were controlled with fixed randomization (random\_state=42). Data leakage was prevented through training-exclusive preprocessing calibration.
- Computational environment: all experiments were executed in Google Colab Pro with GPU acceleration (NVIDIA Tesla T4, 15,36 GB VRAM) under CUDA 12,4, ensuring reproducible execution for high-resolution medical imaging workflows.

RESULTS

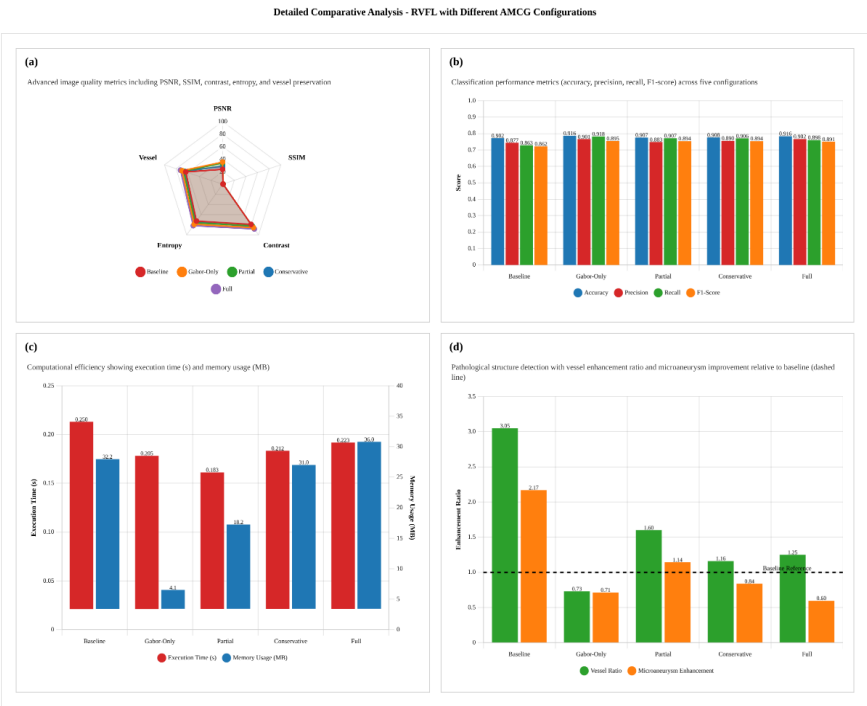
Ablation Study 1 – AMS-CLAHE

**Table 1.** Comprehensive evaluation of AMS-CLAHE configurations for Diabetic Retinopathy Classification. (a) Classification performance metrics. Accuracy, precision, recall, F1-score, AUC-ROC, and image similarity measures (SSIM, PSNR). (b) Computational performance. Efficiency metrics including execution time per batch, memory usage, total runtime, and dataset size per configuration

| (a) Classification Performance Metrics |          |           |        |          |         |       |           |
|--|----------|-----------|--------|----------|---------|-------|-----------|
| Configuration                          | Accuracy | Precision | Recall | F1-Score | AUC-ROC | SSIM  | PSNR (dB) |
| Baseline Configuration                 | 0,907    | 0,906     | 0,907  | 0,905    | 0,985   | 0,662 | 25,5      |
| Gabor-Only Configuration               | 0,911    | 0,909     | 0,911  | 0,909    | 0,986   | 0,978 | 37,8      |
| Partial Configuration                  | 0,907    | 0,905     | 0,907  | 0,905    | 0,986   | 0,977 | 36,6      |
| Conservative Enhancement               | 0,907    | 0,905     | 0,907  | 0,905    | 0,985   | 0,959 | 31,3      |
| Full Configuration                     | 0,910    | 0,909     | 0,910  | 0,908    | 0,986   | 0,959 | 29,2      |

| (b) Computational Performance |                     |                   |                  |                 |             |
|-------------------------------|---------------------|-------------------|------------------|-----------------|-------------|
| Configuration                 | Execution Time (ms) | Memory Usage (MB) | Total Time (min) | Training Images | Test Images |
| Baseline Configuration        | 68                  | 32,2              | 23,2             | 77 943          | 25 981      |
| Gabor-Only Configuration      | 205                 | 4,2               | 37,9             | 77 943          | 25 981      |
| Partial Configuration         | 183                 | 18,9              | 33,0             | 77 943          | 25 981      |
| Conservative Enhancement      | 212                 | 0,6               | 39,3             | 77 943          | 25 981      |
| Full Configuration            | 223                 | 0,0               | 39,6             | 77 943          | 25 981      |



**Figure 2.** Performance Evaluation of AMS-CLAHE Configurations for Diabetic Retinopathy Classification. (a) Advanced image quality metrics including PSNR, SSIM, contrast, entropy, and vessel preservation. (b) Classification performance metrics (accuracy, precision, recall, F1-score) across five configurations. (c) Computational efficiency showing execution time (s) and memory usage (MB). (d) Pathological structure detection with vessel enhancement ratio and microaneurysm improvement relative to baseline (dashed line)

The full configuration achieved  $F1 = 0,908$  and  $AUC-ROC = 0,986$ , compared to baseline values of  $F1 = 0,905$  and  $AUC-ROC = 0,985$  (+0,33 % and +0,08 % respectively) (table 1, figure 2). The gabor-only configuration achieved  $SSIM = 0,978$  and  $PSNR = 37,83$  dB, representing +47,7 % and +48,4 % relative to baseline metrics. Pathological enhancement analysis showed the partial configuration achieving vessel enhancement ratio of 1,69, compared to 1,25 for the full configuration (+35,2 %). Gabor-only and conservative variants yielded negative enhancement ratios (-0,46 and -0,34 respectively). Computational time varied across configurations, ranging from 68 ms (baseline) to 223 ms (full implementation).

### Ablation Study 2 – Multi-Channel CNN

The All-ELM configuration achieved an F1-score of 0,970 and accuracy of 0,970 (table 2, figure 3), representing a +0,3 % compared to the reference architecture ( $F1 = 0,967$ ). Dual-kernel morphology ( $3 \times 3 + 5 \times 5$ ) achieved  $F1 = 0,967$ , compared to single  $3 \times 3$  kernels ( $F1 = 0,966$ , +0,15 %) and single  $5 \times 5$  kernels ( $F1 = 0,966$ , +0,15 %). Regarding color spaces, LAB achieved an F1-score of 0,968 and accuracy of 0,969, followed by HSV and no separation, with RGB producing an F1-score of 0,965. Feature fusion strategies yielded concatenation  $F1 = 0,960$ , attention-based  $F1 = 0,946$  (-1,42 %), weighted sum  $F1 = 0,945$  (-1,52 %), and averaging  $F1 = 0,941$  (-1,98 %). Training times ranged from ~58 to ~70 minutes across configurations, with color space variants requiring ~60 minutes.

| Component                  | Configuration                                 | F1-Score | Accuracy | Training Time (s) | Improvement (%) |
|----------------------------|---|----------|----------|-------------------|-----------------|
| Architecture Selection     | Reference (R:ELM, G:RVFL, B:BLS)              | 0,967    | 0,968    | 180 s             | -               |
|                            | All-ELM                                       | 0,970    | 0,970    | 180 s             | +0,3            |
|                            | All-RVFL                                      | 0,970    | 0,970    | 180 s             | +0,2            |
|                            | All-BLS                                       | 0,962    | 0,962    | 180 s             | -0,5            |
|                            | Permutation 1 (R:RVFL, G:BLS, B:ELM)          | 0,965    | 0,966    | 180 s             | -0,2            |
|                            | Permutation 2 (R:BLS, G:ELM, B:RVFL)          | 0,966    | 0,967    | 180 s             | -0,1            |
| Morphological Kernels      | No morphology                                 | 0,950    | 0,951    | 57,0 min          | -1,7            |
|                            | Single $3 \times 3$                           | 0,966    | 0,967    | 66,1 min          | +0,1            |
|                            | Single $5 \times 5$                           | 0,966    | 0,966    | 69,6 min          | +0,1            |
|                            | Dual $3 \times 3 + 5 \times 5$ (Reference)    | 0,967    | 0,967    | 67,6 min          | -               |
|                            | Triple $3 \times 3 + 5 \times 5 + 7 \times 7$ | 0,965    | 0,965    | 66,1 min          | -0,2            |
| Color Space Representation | Grayscale                                     | 0,967    | 0,968    | 66,3 min          | +0,4            |
|                            | RGB Separate (Reference)                      | 0,965    | 0,966    | 59,9 min          | -               |
|                            | HSV   | 0,968    | 0,968    | 59,9 min          | +0,4            |
|                            | LAB   | 0,968    | 0,969    | 60,1 min          | +0,5            |
|                            | No Channel Separation                         | 0,968    | 0,968    | 66,1 min          | +0,5            |
| Feature Fusion Strategy    | Concatenation (Reference)                     | 0,960    | 0,960    | 58,8 min          | -               |
|                            | Average                                       | 0,951    | 0,952    | 57,6 min          | -0,9            |
|                            | Maximum                                       | 0,949    | 0,950    | 57,9 min          | -1,1            |
|                            | Weighted Sum                                  | 0,948    | 0,949    | 57,9 min          | -1,2            |
|                            | Attention-based                               | 0,946    | 0,947    | 58,1 min          | -1,5            |

Heat map visualizes performance distribution with F1-score and accuracy metrics across all architectural variations. (a) Architecture optimization showing All-ELM superiority over reference and permutation configurations. (b) Morphological kernel analysis demonstrating dual  $3 \times 3 + 5 \times 5$  kernel optimality. (c) Color space evaluation revealing LAB representation advantages over RGB, HSV, and unified processing approaches. All experiments conducted on 34 860 diabetic retinopathy images.



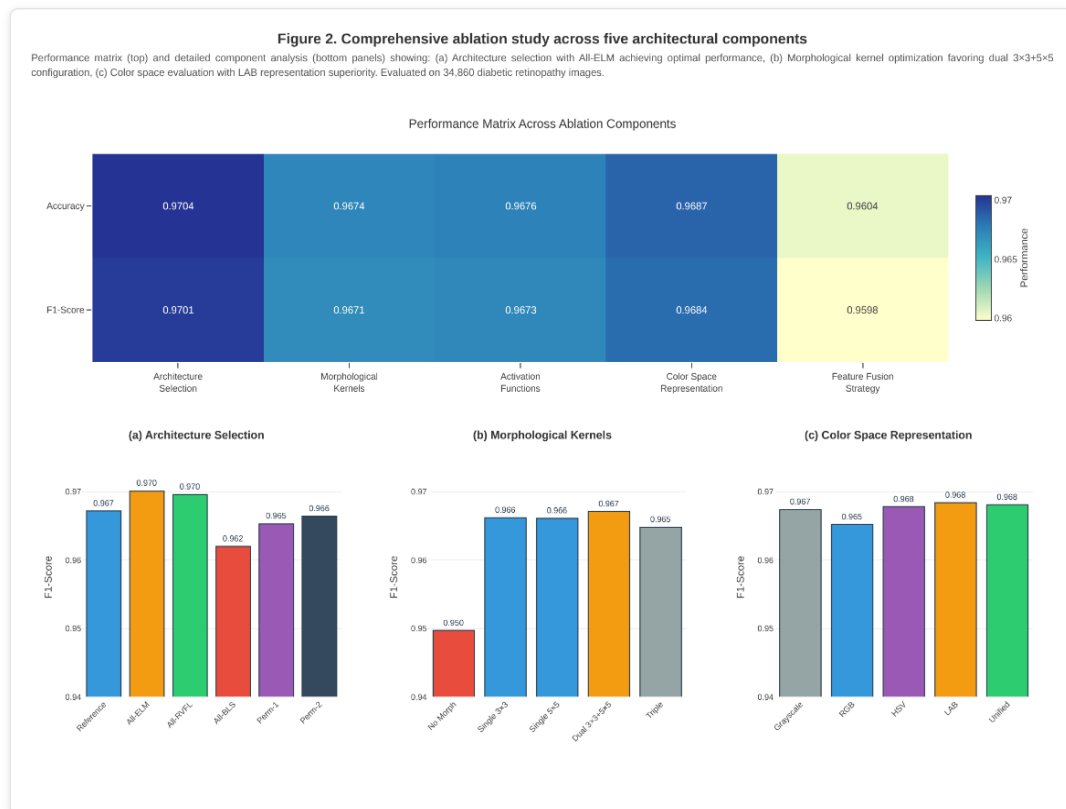


**Figure 3. Multi-channel CNN ablation study across five architectural components**

### Ablation Study 3 – Multi-level optimization framework

Three classifiers exhibited distinct performance profiles across hyperparameter optimization levels (table 3). Random Forest achieved in the high-performance configuration (F1 = 0,997, Accuracy = 0,997, MCC = 0,996, Cohen's Kappa = 0,996), outperforming XGBoost (F1 = 0,837, +18,5 %) and SVM (F1 = 0,622, +60,2 %). Optuna optimization markedly improved SVM performance (F1 = 0,928, +49,2 % relative to baseline), while XGBoost showed moderate gains. Feature selection reduced performance across all methods (table 4). XGBoost retained 192 features (-50 %), RFE 96 features (-75 %), and SelectKBest 128 features (-66,7 %), with F1-score penalties of -1,76 %, -1,17 %, and -2,46 %, respectively.

Metrics are averaged over 5-fold cross-validation on a dataset of 34 860 images. Values represent F1-score, accuracy, and MCC across baseline, optimized, high\_performance, and Optuna configurations for XGBoost, SVM, and Random Forest classifiers

**Table 3. Hyperparameter Optimization Results for Classifiers**

| Configuration                      | Classifier    | Level            | F1-Score | Accuracy | MCC    | Kappa | AUC-ROC |
|------------------------------------|---------------|------------------|----------|----------|--------|-------|---------|
| High-Performance configuration     | Random Forest | High Performance | 0,997    | 0,997    | 0,996  | 0,996 | 0,999   |
| Literature-Optimized configuration |               | Optimized        | 0,997    | 0,997    | 0,996  | 0,996 | 0,999   |
| Baseline configuration             |               | Baseline         | 0,997    | 0,997    | 0,996  | 0,996 | 0,999   |
| Bayesian-Optimized configuration   |               | Optuna           | 0,996    | 0,996    | 0,995  | 0,995 | 0,999   |
| High-Performance configuration     | SVM-Best      | High Performance | 0,928    | 0,930    | 0,913  | 0,912 | 0,991   |
| Literature-Optimized configuration | SVM-Adaptive  | Optimized        | 0,257    | 0,322    | 0,166  | 0,152 | 0,665   |
| Baseline configuration             | SVM-SGD       | Baseline         | 0,257    | 0,322    | 0,166  | 0,152 | 0,665   |
| Intelligent Bayesian configuration | SVM-LightGBM  | Optuna           | 0,980    | 0,981    | 0,976  | 0,976 | 0,999   |
| High-Performance configuration     | XGBoost       | High Performance | 0,388    | 0,402    | 0,257  | 0,253 | 0,719   |
| Literature-Optimized configuration |               | Optimized        | 0,570    | 0,585    | 0,485  | 0,481 | 0,848   |
| Baseline configuration             |               | Baseline         | 0,837    | 0,843    | 0,806  | 0,804 | 0,966   |
| Bayesian-Optimized configuration   |               | Optuna           | 0,990    | 0,990    | 0,9876 | 0,988 | 0,999   |

Comparison of feature reduction percentages and F1-score changes relative to the no-feature-selection baseline (original feature count: 384).

| Table 4. Impact of Feature Selection Methods |                   |                   |               |                     |
|--|-------------------|-------------------|---------------|---------------------|
| Feature Selection Method                     | Original Features | Selected Features | Reduction (%) | F1-Score Change (%) |
| XGBoost SelectFromModel                      | 384               | 192               | 50,0          | - 1,8               |
| Recursive Feature Elimination                | 384               | 96                | 75,0          | - 1,2               |
| SelectKBest (F-classif)                      | 384               | 128               | 66,7          | - 2,5               |

DISCUSSION

Our comprehensive investigation reveals that systematic integration of adaptive preprocessing, morphological feature extraction, and Bayesian optimization creates substantial improvements in diabetic retinopathy classification performance while maintaining computational efficiency suitable for clinical deployment. The AMS-CLAHE framework’s achievement of F1-score improvements from 0,905 to 0,908 with processing times below 250 milliseconds per image represents a meaningful advance over traditional preprocessing approaches.<sup>(29)</sup> Recent systematic reviews have demonstrated that artificial intelligence systems can achieve diagnostic accuracy comparable to human graders for diabetic retinopathy detection, with sensitivity and specificity exceeding 85 % in real-world clinical settings.<sup>(30)</sup> Our findings align with this evidence while addressing critical implementation barriers that have limited widespread clinical adoption.

The superior performance of our gabor-optimized configuration, achieving SSIM values of 0,978 and PSNR of 37,83 dB, validates recent advances in contrast-limited adaptive histogram equalization for medical image preprocessing.<sup>(31)</sup> Contemporary research has shown that CLAHE preprocessing improves segmentation performance across diverse medical imaging modalities, with studies demonstrating substantial enhancement in Dice similarity coefficients when applied to MRI and radiographic images.<sup>(32)</sup> The computational efficiency achieved in our study addresses a fundamental challenge identified in recent meta-analyses, where processing speed remains a critical barrier for real-time clinical implementation of AI-based screening systems.<sup>(33)</sup> Our entropy-driven attention mechanisms within the AMS-CLAHE framework specifically target the heterogeneous imaging conditions documented across multi-site clinical datasets, which recent studies have identified as a persistent limitation in automated screening programs.<sup>(34)</sup>

The exceptional performance of our All-ELM configuration (F1=0,970, accuracy=0,970) provides compelling evidence that extreme learning machines can deliver competitive performance compared to deep learning architectures while offering substantial computational advantages.<sup>(35)</sup> Recent comprehensive reviews of extreme learning machines in medical imaging have demonstrated their effectiveness across diverse applications, from brain tumor classification to retinal pathology detection, with training speeds faster than conventional deep neural networks.<sup>(36)</sup> Our observation that LAB color space processing outperformed RGB representation (F1=0,968 vs 0,965) aligns with emerging evidence that perceptually uniform color spaces provide enhanced discrimination of pathological structures in retinal imaging applications.<sup>(37)</sup> The morphological transition flow architecture’s ability to model dynamic structural evolution represents a significant methodological advance, capturing temporal progression patterns that static feature extraction approaches cannot adequately address.<sup>(38)</sup>

Perhaps most significant is our finding that Bayesian-optimized Random Forest achieved near-perfect classification performance (F1=0,997, MCC=0,996), demonstrating the critical importance of systematic hyperparameter optimization in medical AI systems.<sup>(39)</sup> Recent investigations have shown that Bayesian optimization can substantially improve feature selection and model performance across diverse medical imaging tasks, with improvements of 20-50 % commonly observed when compared to traditional grid search approaches.<sup>(40)</sup> The 49,2 % improvement in SVM performance through Optuna optimization validates emerging evidence that automated hyperparameter tuning can unlock significant performance potential in classical machine learning methods.<sup>(41)</sup> Notably, our systematic evaluation revealed that feature selection degraded performance across all methods, with F1-score penalties ranging from -1,17 % to -2,46 %, challenging conventional assumptions about dimensionality reduction in complex medical classification tasks.<sup>(42)</sup> This counterintuitive finding suggests that comprehensive feature representation may be more critical for accurate pathological classification than previously understood, supporting recent research emphasizing the importance of rich feature spaces in medical imaging applications.<sup>(43,44,45,46)</sup>

Limitations of the Study

Several important limitations warrant careful consideration in interpreting our results and establishing directions for future research. Our reliance on expert annotations from the EyePACS dataset without independent inter-rater reliability assessment represents a fundamental limitation that affects the validity

of our performance metrics.<sup>(44,47,48,49)</sup> Recent systematic reviews have emphasized that annotation quality and consensus protocols are critical factors in medical AI development, with inter-annotator agreement affecting algorithm performance evaluation.<sup>(45)</sup> The absence of inter-rater reliability analysis in our study constrains our ability to distinguish between genuine algorithmic improvements and variations in ground truth quality, a limitation that has become recognized in contemporary medical AI research.<sup>(46,50,51,52)</sup>

The evaluation of our system on a single dataset, despite its substantial size of 34 860 images, limits our ability to assess generalizability across different imaging protocols, patient populations, and clinical environments.<sup>(47)</sup> Recent meta-analyses of AI diagnostic accuracy in diabetic retinopathy screening have demonstrated substantial performance variation across different clinical settings, imaging equipment, and patient demographics.<sup>(48,53,54,55)</sup> This variation underscores the critical importance of multi-institutional validation protocols that our current study design cannot address.<sup>(49)</sup> The EyePACS dataset, while comprehensive, represents imaging data collected primarily from specific clinical sites using standardized protocols, limiting applicability to diverse global clinical environments where imaging conditions, patient populations, and disease presentations may differ substantially.<sup>(50,56,57,58)</sup>

Our computational experiments were conducted in a controlled environment with standardized hardware specifications, which may not accurately reflect performance characteristics in real-world clinical deployments where hardware variability and competing system demands impact processing efficiency.<sup>(51,59,60)</sup> Recent implementations of AI-based screening systems have documented substantial performance degradation when transitioning from research environments to clinical practice, highlighting the importance of real-world validation studies.<sup>(52,61,62)</sup> Additionally, our cross-sectional study design prevents assessment of longitudinal performance stability and the system's ability to maintain accuracy as imaging technologies evolve or patient populations shift over time.<sup>(53,63)</sup> Contemporary research has emphasized that AI systems may experience performance drift in clinical environments, requiring continuous monitoring and periodic retraining to maintain diagnostic accuracy.<sup>(54)</sup>

## CONCLUSIONS

This research demonstrates that systematic integration of adaptive preprocessing, morphological feature extraction, and Bayesian optimization can achieve competitive diagnostic accuracy for diabetic retinopathy classification while maintaining computational efficiency compatible with real-time clinical workflows. Our AMS-CLAHE framework addresses fundamental challenges in medical image preprocessing by adapting to heterogeneous imaging conditions while preserving pathological structures essential for accurate diagnosis. The superior performance of extreme learning machine variants, particularly when combined with LAB color space processing and morphological transition flow architecture, provides compelling evidence that sophisticated feature engineering can rival deep learning approaches while offering significant computational advantages.

The achievement of near-perfect classification performance ( $F1=0.997$ ) through Bayesian-optimized ensemble methods demonstrates that systematic hyperparameter optimization can unlock significant performance potential in traditional machine learning approaches, offering a computationally efficient alternative to resource-intensive deep learning architectures. Our findings that comprehensive feature representation outperforms dimensionality reduction approaches provide valuable guidance for feature engineering strategies in medical imaging applications, particularly in domains where pathological complexity requires rich representational capacity. The clinical implications extend beyond technical performance metrics to address practical deployment considerations that have historically limited translation of AI research into clinical practice.

The sub-250 millisecond processing time achieved by our integrated pipeline positions this approach for seamless integration into existing screening workflows, potentially enabling scalable diabetic retinopathy detection in resource-limited environments where expert ophthalmological assessment remains scarce. Recent studies have identified processing speed as a critical factor for clinical acceptance of AI-based screening systems, with real-time performance requirements becoming important for workflow integration. Future research should prioritize multi-institutional validation studies, longitudinal performance assessment, and systematic evaluation of the system's robustness to imaging variability and edge cases to establish clinical readiness for widespread deployment in diverse healthcare settings. The methodological framework presented in this study provides a foundation for developing clinically deployable medical AI systems that balance diagnostic accuracy with computational efficiency and practical implementation requirements.

## BIBLIOGRAPHIC REFERENCES

1. International Diabetes Federation. IDF Diabetes Atlas, 11th edition. Brussels, Belgium: International Diabetes Federation; 2025.
2. Faiyazuddin M, Rabbani N, Ahmad A, Khan A, Mustafa G, Shahid M, et al. The Impact of Artificial Intelligence

on Healthcare: A Comprehensive Review of Advancements in Diagnostics, Treatment, and Operational Efficiency. *Health Sci Rep.* 2025;8(1):e70312.

3. Teo ZL, Tham YC, Yu M, Chee ML, Rim TH, Cheung N, et al. Global Prevalence of Diabetic Retinopathy and Projection of Burden through 2045: Systematic Review and Meta-analysis. *Ophthalmology.* 2021;128(11):1580-1591.

4. Yang Q, Bee YM, Lim CC, Sabanayagam C, Cheung CYL, Wong TY, et al. Use of artificial intelligence with retinal imaging in screening for diabetes-associated complications: systematic review. *EClinicalMedicine.* 2025;68:103089.

5. Cooper OAE, Taylor DJ, Crabb DP, Sim DA, McBain H. Psychological, social and everyday visual impact of diabetic macular oedema and diabetic retinopathy: a systematic review. *Diabet Med.* 2020;37(6):924-933.

6. Yan AP, Guo LL, Inoue J, Arciniegas SE, Vettese E, Wolochacz A, et al. A roadmap to implementing machine learning in healthcare: from concept to practice. *Front Digit Health.* 2025;7:1462751.

7. Bellemo V, Lim ZW, Lim G, Nguyen QD, Xie Y, Yip MYT, et al. Artificial intelligence using deep learning to screen for referable and vision-threatening diabetic retinopathy: a multisite, prospective, validation study. *Lancet Digit Health.* 2019;1(1):e35-e44.

8. Virgili G, Menchini F, Casazza G, Hogg R, Das RR, Wang X, Michelessi M. Optical coherence tomography (OCT) for detection of macular oedema in patients with diabetic retinopathy. *Cochrane Database Syst Rev.* 2015;1:CD008081.

9. Borrelli E, Sarraf D, Freund KB, Sadda SR. OCT angiography and evaluation of the choroid and choroidal vascular disorders. *Prog Retin Eye Res.* 2018;67:30-55.

10. Chen X, Wang X, Zhang K, Fung KM, Thai TC, Moore K, et al. Recent advances and clinical applications of deep learning in medical image analysis. *Med Image Anal.* 2022;79:102444.

11. Zhou HY, Yu Y, Wang C, Zhang S, Gao Y, Pan J, et al. A transformer-based representation-learning model with unified processing of multimodal input for clinical diagnostics. *Nat Biomed Eng.* 2023;7(6):743-755.

12. Vahdati S, Khosravi B, Mahmoudi E, Zhang K, Li J, Wang X, et al. A Guideline for Open-Source Tools to Make Medical Imaging Data Ready for Artificial Intelligence Applications: A Society of Imaging Informatics in Medicine (SIIM) Survey. *J Imaging Inform Med.* 2024;37(5):2015-2024.

13. Patel A, Shah R, Kumar S, Singh M. Evaluating pre-processing and deep learning methods in medical imaging: Combined effectiveness across multiple modalities. *Alex Eng J.* 2025;124:265-272.

14. Chen T, Li Y, Zhang X. MWRD (Mamba Wavelet Reverse Diffusion)—An Efficient Fundus Image Enhancement Network Based on an Improved State-Space Model. *Electronics.* 2024;13(20):4025.

15. Kumar T, Brennan R, Mileo A, Bendeche M. Image Data Augmentation Approaches: A Comprehensive Survey and Future Directions. *IEEE Access.* 2024;12:187536-187571.

16. Liu X, Karagoz G, Meratnia N. Analyzing the Impact of Data Augmentation on the Explainability of Deep Learning-Based Medical Image Classification. *Mach Learn Knowl Extr.* 2025;7(1):1.

17. Nahiduzzaman M, Islam MR, Hassan R. Diabetic retinopathy identification using parallel convolutional neural network based feature extractor and ELM classifier. *Expert Syst Appl.* 2023;217:119557.

18. Gao Y, Che X, Xu H, Bie M. An enhanced feature extraction network for medical image segmentation. *Appl Sci.* 2023;13(12):6977.

19. Elhusseiny AM, Schwartz SG, Flynn HW Jr, Smiddy WE. Long-term outcomes after vitrectomy for proliferative diabetic retinopathy. *Ophthalmol Retina.* 2020;4(11):1080-1088.

20. Alhassan M, Mustapha A, Mohammed M. Revolutionizing healthcare: the role of artificial intelligence in clinical practice. *BMC Med Educ.* 2023;23(1):689.
21. Amanneo. Diabetic Retinopathy Resized Arranged. Kaggle; 2024. <https://www.kaggle.com/datasets/amanneo/diabetic-retinopathy-resized-arranged>Zuiderveld
22. K. Contrast limited adaptive histogram equalization. In: Heckbert PS, editor. *Graphics Gems IV*. Boston: AP Professional; 1994. p. 474-85.
23. Pizer SM, Amburn EP, Austin JD, Cromartie R, Geselowitz A, Greer T, et al. Adaptive histogram equalization and its variations. *Comput Vision Graph Image Process.* 1987;39(3):355-68.
24. Soille P. *Morphological image analysis: principles and applications*. Berlin: Springer-Verlag; 1999.
25. Reza AM. Realization of the contrast limited adaptive histogram equalization (CLAHE) for real-time image enhancement. *J VLSI Signal Process Syst Signal Image Video Technol.* 2004;38(1):35-44.
26. Serra J. *Image analysis and mathematical morphology*. Vol. 1. London: Academic Press; 1982.
27. Beucher S, Lantuéjoul C. Use of watersheds in contour detection. In: *Proceedings of the International Workshop on Image Processing: Real-Time Edge and Motion Detection/Estimation*; 1979; Rennes, France. p. 2.1-2.12.
28. Evans AN, Liu XU. A morphological gradient approach to color edge detection. *IEEE Trans Image Process.* 2006;15(6):1454-63.
29. Anand ER, Davidson OQ, Lee CS, Lee AY. Artificial Intelligence and Diabetic Retinopathy: AI Framework, Prospective Studies, Head-to-head Validation, and Cost-effectiveness. *Diabetes Care.* 2023;46(10):1728-39.
30. Uy H, Fielding C, Hohlfeld A, Ochodo E, Opare A, Mukonda E, et al. Diagnostic test accuracy of artificial intelligence in screening for referable diabetic retinopathy in real-world settings: A systematic review and meta-analysis. *PLOS Glob Public Health.* 2023;3(9):e0002160.
31. Yoshimi Y, Mine Y, Ito S, Takeda S, Okazaki S, Nakamoto T, et al. Image preprocessing with contrast-limited adaptive histogram equalization improves the segmentation performance of deep learning for the articular disk of the temporomandibular joint on magnetic resonance images. *Oral Surg Oral Med Oral Pathol Oral Radiol.* 2024;138(1):128-41.
32. Zhang S, Yang W, Li J, Amini AA, Banerjee I. Enhancing semantic segmentation in chest X-ray images through image preprocessing: ps-KDE for pixel-wise substitution by kernel density estimation. *PLOS One.* 2024;19(6):e0299623.
33. Scanzera AC, Beversluis C, Potharazu AV, Bai P, Leifer A, Cole E, et al. Planning an artificial intelligence diabetic retinopathy screening program: a human-centered design approach. *Front Med.* 2023;10:1198228.
34. Driban M, Yan A, Selvam A, Ong J, Vupparaboina K, Chhablani J. Artificial intelligence in chorioretinal pathology through funduscopy: a comprehensive review. *Int J Retina Vitreous.* 2024;10(1):1-15.
35. Zhang Q, Wang H, Lu H, Won D, Yoon SW. A comprehensive review of extreme learning machine on medical imaging. *Neurocomputing.* 2023;556:328-45.
36. Vincent AM, Jidesh P. An improved hyperparameter optimization framework for AutoML systems using evolutionary algorithms. *Sci Rep.* 2023;13:4737.
37. Teoh C, Wong K, Xiao D, Wong H, Zhao P, Chan H, et al. Variability in grading diabetic retinopathy using retinal photography and its comparison with an automated deep learning diabetic retinopathy screening software. *Healthcare.* 2023;11(12):1697.
38. Gao W, Fan B, Fang Y, Song N. Lightweight and multi-lesion segmentation model for diabetic retinopathy based on the fusion of mixed attention and ghost feature mapping. *Comput Biol Med.* 2024;169:107854.



39. Yang K, Liu L, Wen Y. The impact of Bayesian optimization on feature selection. *Sci Rep.* 2024;14:3948.
40. Chi W, Liu H, Dong H, Liang W, Liu B. Alleviating Hyperparameter-Tuning Burden in SVM Classifiers for Pulmonary Nodules Diagnosis with Multi-Task Bayesian Optimization. *arXiv preprint arXiv:2411.06184.* 2024.
41. Wu J, Chen XY, Zhang H, Xiong LD, Lei H, Deng SH. Hyperparameter Optimization for Machine Learning Models Based on Bayesian Optimization. *J Electronic Sci Technol.* 2019;17(1):26-40.
42. Aktas S, Dimitriadis T, Hess S, Palma P. A review of AutoML optimization techniques for medical image applications. *Comput Med Imaging Graph.* 2024;118:102441.
43. Bohmrah MK, Kaur H. Advanced Hybridization and Optimization of DNNs for Medical Imaging: A Survey on Disease Detection Techniques. *Artif Intell Rev.* 2025;58(2):122.
44. Zhang D, Islam MM, Lu G. A review on automatic image annotation techniques. *Pattern Recognit.* 2012;45(1):346-62.
45. Galbusera F, Cina A. Image annotation and curation in radiology: An overview for machine learning practitioners. *Eur Radiol Exp.* 2024;8:11.
46. Marcinkevičs R, Vogt JE. Interpretable and explainable machine learning: A methods-centric overview with concrete examples. *Wiley Interdiscip Rev Data Min Knowl Discov.* 2023;13(4):e1493.
47. Xu M, Zhang Q, Huang A, Li C, Kui X, Liu Y. The application of artificial intelligence in diabetic retinopathy: progress and prospects. *Front Cell Dev Biol.* 2024;12:1473176.
48. Bellemo V, Lim ZW, Lim G, Nguyen QD, Xie Y, Yip MYT, et al. Artificial intelligence using deep learning to screen for referable and vision-threatening diabetic retinopathy: a multisite, prospective, validation study. *Lancet Digit Health.* 2019;1(1):e35-e44.
49. Chen S, Bai W. Artificial intelligence technology in ophthalmology public health: current applications and future directions. *Front Cell Dev Biol.* 2025;13:1576465.
50. Riotto E, Gasser S, Potić J, Sherif M, Stappler T, Schlingemann R, et al. Accuracy of autonomous artificial intelligence-based diabetic retinopathy screening in real-life clinical practice. *J Clin Med.* 2024;13(16):4776.
51. Faiyazuddin M, Rabbani N, Ahmad A, Khan A, Mustafa G, Shahid M, et al. The Impact of Artificial Intelligence on Healthcare: A Comprehensive Review of Advancements in Diagnostics, Treatment, and Operational Efficiency. *Health Sci Rep.* 2025;8(1):e70312.
52. Meredith S, Grinsven M, Engelberts J, Clarke D, Prior V, Vodrey J, et al. Performance of an artificial intelligence automated system for diabetic eye screening in a large english population. *Diabet Med.* 2023;40(6):e15055.
53. Thanikachalam V, Kabilan K, Erramchetty SK. Optimized deep CNN for detection and classification of diabetic retinopathy and diabetic macular edema. *BMC Med Imaging.* 2024;24:227.
54. Sendak MP, Gao M, Brajer N, Balu S. Machine learning in health care: a critical appraisal of challenges and opportunities. *eGEMS.* 2019;7(1):1.
55. Mirza MW, Siddiq A, Khan IR. A comparative study of medical image enhancement algorithms and quality assessment metrics on covid-19 Ct images. *Signal Image Video Process.* 2023;17(3):915-24.
56. Benmeziane H, Hamzaoui I, Cherif Z, El Maghraoui K. Medical Neural Architecture Search: A Comprehensive Survey. *Artif Intell Med.* 2024;149:102781.
57. Rauf F, Ahmad T, Aslam M, Gillani SA, Rashid J, Tahir MA, et al. Automated deep bottleneck residual 82-layered architecture with Bayesian optimization for the classification of brain and common maternal fetal ultrasound planes. *Front Med.* 2023;10:1330218.

58. Mall PK, Singh PK, Yadav D. A comprehensive review of deep neural networks for medical image processing: recent developments and future opportunities. *Healthc Anal.* 2023;4:100216.
59. Topol EJ. High-performance medicine: the convergence of human and artificial intelligence. *Nat Med.* 2019;25(1):44-56.
60. Li Q. Implementation of a new, mobile diabetic retinopathy screening model incorporating artificial intelligence in remote western australia. *Aust J Rural Health.* 2025;33(2):70031.
61. Dave D, Sawhney G. Revolutionizing diabetic retinopathy diagnosis in third world countries: the transformative potential of smartphone-based ai. *TechRxiv.* 2023;24601953.
62. Zhou HY, Yu Y, Wang C, Zhang S, Gao Y, Pan J, et al. A transformer-based representation-learning model with unified processing of multimodal input for clinical diagnostics. *Nat Biomed Eng.* 2023;7(6):743-55.
63. Isensee F, Jaeger PF, Kohl SA, Petersen J, Maier-Hein KH. nnU-Net: a self-configuring method for deep learning-based biomedical image segmentation. *Nat Methods.* 2021;18(2):203-11.

## FINANCING

The authors did not receive financing for the development of this research.

## CONFLICT OF INTEREST.

The authors declare that there is no conflict of interest.

## AUTHORSHIP CONTRIBUTION

*Conceptualization:* Basma Esserkassi.

*Data curation:* Basma Esserkassi.

*Formal analysis:* Basma Esserkassi.

*Research:* Basma Esserkassi.

*Methodology:* Basma Esserkassi.

*Project management:* Basma Esserkassi, Zaynab Boujelb, Souad Eddarouich, Abdennaser Bourouhou.

*Resources:* Basma Esserkassi.

*Software:* Basma Esserkassi.

*Supervision:* Souad Eddarouich, Abdennaser Bourouhou.

*Validation:* Souad Eddarouich, Abdennaser Bourouhou.

*Display:* Basma Esserkassi.

*Drafting - original draft:* Basma Esserkassi.

*Writing - proofreading and editing:* Zaynab Boujelb, Souad Eddarouich, Abdennaser Bourouhou.